TRANSPORTES
revistatransportes.org.br
anpet
associação nacional de pesquisa e ensino em transportes
anpet.org.br

Use of ultrasonic tomography for the assessment of critical aspects of doweled joints in concrete pavements

Utilização da tomografia ultrassônica para avaliação dos aspectos críticos de barras em juntas de pavimentos de concreto

Eric Ribeiro da Silva[1], **José Tadeu Balbo**[2], **Andréia Posser Cargnin**[3]

[1]University of São Paulo, São Paulo – Brazil, eric_83@usp.br
[2]University of São Paulo, São Paulo – Brazil, jotbalbo@usp.br
[3]University of São Paulo, São Paulo – Brazil, andreiacargnin@usp.br

Submitted:
11 de maio de 2022
Accepted for publication:
21 de agosto de 2022
Published:
13 de dezembro de 2022
Editor in charge:
Francisco Sacramento Aragão

Keywords:
Ultrasonic tomography.
Concrete pavement.
Bar misalignment.

Palavras-chave:
Tomografia ultrassônica.
Pavimentos de concreto.
Desalinhamento de barras.

DOI:10.14295/transportes.v30i3.2772

ABSTRACT
The critical (design) parameters to be controlled for concrete pavements construction, in addition to the concrete strength, are slab`s thicknesses and doweled bars position at contraction joints, as they affect hugely structural performance, and, if not properly built may cause early ruptures. Construction compliance of such parameters is nowadays assessed through nondestructive techniques (NDT), such as ultrasonic low-frequency waves. Alignments of inserted doweled bars at contraction joints are analyzed herein for actual slabs as well as how thickness affects such position. Tests were carried out over an airport hangar apron after it has been built. Twenty-five concrete slabs were assessed using ultrasonic tomography allowing to verify disconformities of thicknesses and bars vertical and horizontal misalignments, with fair accuracy on measuring deviation angles of bars.

RESUMO
Os parâmetros (de projeto) críticos a serem controlados na construção de pavimentos de concreto simples, além da resistência do concreto, são as espessuras das placas e o posicionamento das barras de transferência de cargas em juntas, pois afetam sobremaneira o desempenho estrutural podendo, por falhas, ocasionar rupturas precoces. A determinação da conformidade construtiva desses parâmetros é contemporaneamente realizada por meio de métodos não destrutivos (NDT), como a tomografia de ondas de baixa frequência. Analisa-se neste artigo a adequação do alinhamento das barras de transferência de cargas em juntas e como variações na espessura do concreto o afetam. O pavimento selecionado para os testes foi o pátio de hangar aeroportuário pouco após sua construção. Vinte e cinco placas de concreto foram avaliadas quanto às variáveis mencionadas, tendo sido possível observar desuniformidades de espessuras bem como desalinhamentos verticais e horizontais de barras de aço em juntas, permitindo tal NDT acurácia razoável na determinação dos ângulos de desvio de barras em juntas de contração.

1. INTRODUCTION

The inspection of concrete pavement thickness is usually performed through sample`s coring, allowing to analyze the concrete slab thickness based on a limited number of samples (due to the extraction costs and time-consuming). The same can be stated to past methods for checking dowel bar's location, length, and amount in transversal joints, requiring destructive inspections

when under suspicious situation. In addition, since they are destructive methods, their productivity is low. Also, demands a subsequent repair at any positions wherever the samples were extracted.

Moreover, one should note that the limited number of samples obtained at each slab when coring the pavement might impair the assessment of constructive failures such as lack of uniformity in the slabs thickness. It occurs, mostly, because of the standards permissiveness, in some countries, regarding the employment of techniques and equipment uncapable to ensure a suitable flatness for the before built base layer, usually a roller compacted concrete (RCC) or cement-treated crushed stones (CTCS).

Balbo (2014), for instance, presented (through sample's coring) a significant variation in the slab thickness of a concrete pavement placed with a slipform paver; the thickness ranged from 175 mm to 314 mm, whereas the design specification was 230 mm. The author states that such variations are associated to the base material (RCC) spreading with a motor grader, leading to base layer finishing flaws and superficial unevenness.

Also, according to Balbo (2014), it is necessary to fix ways to mitigate the concrete slab thickness variation, seeking to reduce the slabs degradation risk, since the fatigue phenomenon is quite sensible to thickness variations. Effective load transfer between joints is of main concern to airport infrastructure and it depends not only on bar alignment as well as on the concrete temperature and the underneath asphalt or compacted concrete base to bear and transfer the aircraft gear loads (Federal Aviation Administration, 2021). Paramount concern is also given to slabs full doweled (both longitudinal and transversal joints) when movement locking could be even more critical compared to slabs with conventional longitudinal tie bars.

Concerning the inspection of dowel bars position, Gancarz *et al*. (2015) describes that, in the past, albeit the dowel bars misalignment (Figure 1) was considered matter of concern, the transportation agencies did not conduct inspections to check the dowel bars orientation after concrete placement. According to Tayabji (1986) and Rao *et al*. (2009), inspections of dowel bars location after construction were not conducted due to the lack of practical protocols.

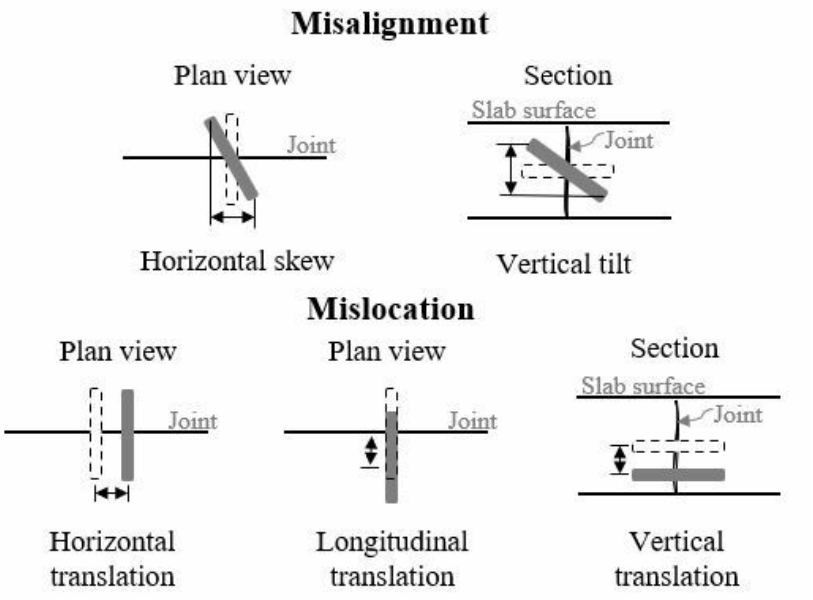

Figure 1. Types of dowel bars misalignments and misallocations (Adapted from Tayabji, 1986)

The main concern about the dowel bars proper positioning is related to the risk of locking the joint. Although the incidence of one dowel bar sharply misaligned is not reason of concern, if several dowel bars in the same joint present significant misalignments, the risk of joint locking is increased (STUGES *et al.*, 2014).

According to the Federal Highway Administration (FHWA, 2018) the locking of an individual joint would not affect the pavement performance. However, the locking of successive joints increases the risk of breaking the slab due to movement restriction during the concrete expansion and contraction ascribed to seasonal and daily thermal and moisture oscillations, resulting, consequently, in the malfunction of the system, which may lead to transverse cracks parallel to the joints.

For these reasons, seeking to reduce the incidence of problems related to joints malfunction, most of the road agencies usually establish tolerances on the precision of dowel bars positioning and alignment. However, according to the American Concrete Pavement Association (ACPA, 2006), despite these tolerances can be considered strict, these patterns are not usually related to the pavement performance in field.

In Brazil (DNIT, 2013) deviations of the dowel bar end of ±1% based on its length are allowed as long as at least two thirds of the dowel bars, at the same joint, do not present deviations higher than ±0.7%. Such limits arbitrarily adopted are too conservative when compared to the limits admitted in countries with strong tradition of concrete pavement construction, like United States and Germany, as depicted in Table 1.

Table 1 – Tolerances on the dowel bars position and alignment

Country	Vertical tilt	Horizontal skew	Longitudinal translation	Vertical translation	Source
Brazil	1.0%	1.0%	1.0%	1.0%	DNIT (2013)
Germany	4.2%	4.2%	11.1%	-	*Rao et al.* (2009)
USA	3.3%	3.3%	11.1%	5.6%*	FHWA (2007); ACPA (2013)

*It is required concrete minimum covering of 75 mm from the top and bottom of the slab.

Tolerances for dowel bars misalignments in Brazil are like the British ones at the early 1970s (PARMENTER, 1973). According to the author, the dowel bars misalignment tolerances before the concrete pouring were: 1% of rotational misalignment (horizontal or vertical) of one third of the bars at the joint; the other two thirds of bars should be within a tolerance of 0.5%; and no dowel bar should differ in alignment from the adjacent one in more than 1.0%.

Parmenter (1973) verified the position of dowel bars in field through removal of concrete still fresh to reevaluate the bars alignment and coring samples of hardened concrete with 100 mm of diameter at both ends of the bars. In this study, the author pointed out the tolerances afore mentioned were overly rigid and misalignments of 3% and 4% would be acceptable. This already demonstrated the need for reviewing the acceptance criteria based on field performance data.

In the present study, the MIRA ultrasonic tomography device was used to assess a newly built concrete pavement in an airport apron, mainly aiming to evaluate the equipment applicability to pinpoint the dowel bars, besides measuring the concrete slabs thickness to improve the understanding about the reasons for bars misalignments.

2. MIRA ULTRASONIC TOMOGRAPHY DEVICE

Among the current techniques for non-destructive tests (NDT), ultrasonic tomography stands

out for enabling to check concrete slabs thickness, inspect the position of embedded elements like longitudinal reinforcement and dowel bars, as well as the incidence of distresses such as cracks and delamination.

On ultrasonic tomography devices have transducers generating sound waves which are sent and reflected at the interface of materials with different acoustic impedances. The details about the signal propagation through a material are derived from the analysis of the reflected signal and can be found elsewhere (HOEGH *et al*., 2011; LYBAERT, 2015).

Because of the high difference on the air and concrete acoustic impedance, mostly of the energy is reflected and almost none is transmitted. Accordingly, an incident ultrasonic pulse is reflected by the concrete heterogeneous structure, resulting in an overlapping of many reflections of the received signal, commonly called as structural noise. Such a noise trends to conceal the object of interest, suppressing its detection (SCHICKERT *et al*., 2003).

The limitations caused by the concrete heterogeneities might be mitigated by using the dry point contact (DPC) ultrasonic tomography, which applies a matrix of paired transducers that send and receive the ultrasound signal (LYBAERT, 2015).

According to Hoegh *et al*. (2011), the use of several pairs of transducers in each scan allows the redundancy of information required to assess heterogeneous media, like Portland cement concrete (PCC). Furthermore, the DPC transducers can transmit elastic waves of low frequency (25 to 85 kHz) capable of penetrating greater depths.

The MIRA equipment (Figure 2) applies the DPC ultrasonic tomography technology for non-destructive assessment of distress or objects embedded in the concrete, like steel (AGUIRRE *et al*., 2013). The equipment is composed of 48 transducers for emission and reception, linearly arranged in 12 channels of 4 transducers; each channel with 4 transducers sends out sequentially shear wave pulses while the other 11 channels receive the reflections of internal interfaces. This arrangement allows 66 separate measurements of transmission-reception transducers per scan (LYBAERT, 2015).

(a) Equipment superior view (b) Pairs of transducers

Figure 2. Ultrasonic tomography device (MIRA)

To calibrate the signal speed of propagation in the material, the device measures the signal propagation time between the transducers and applies the Synthetic Aperture Focusing Technique (SAFT) to analyze and reconstruct (image formation) based on the shear waves reflections (HOEGH *et al*., 2011).

According to Hoegh *et al*. (2012), each MIRA's scan provides a SAFT B-scan with the vertical axis indicating the depth of any reflection (caused by the differences in the acoustic impedance) and the horizontal axis indicating the localization along the device aperture (250 mm). Changes in the acoustic impedance cause a high intensity reflection (red color) associated to the distress position at the B-scan (for instance, interface between layers, damages in the concrete or steel bars), as depicted in the Figure 3.

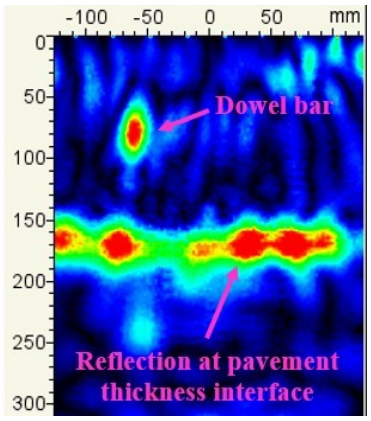

Figure 3. Example of B-scan measurement

2.1. Equipment operating modes

The data acquisition with MIRA can be conducted using two operating modes: the "explore" mode which allows performing tests in arbitrary positions through the B-scans visualizations on the structure; and the "scan" mode applied to create a data folder to store the results of the surface complete scan (mapping) (GERMANN INSTRUMENTS, 2016).

Whilst the explore mode enables localized data acquisition (for instance, at the middle of the concrete slab) in few seconds, the scan mode allows the tridimensional (3-D) reconstruction of the evaluated structure using the software IDealviewer which is an equipment supplement.

However, according to the equipment manual of operation (Germann Instruments, 2016), in the scan mode, the measurement should be taken, at the most, every 250 mm horizontally and every 100 mm vertically, in relation to the device displacement during the data acquisition, allowing to map the studied region for its subsequent reconstruction (as an image).

It is worth noting that the shorter the spacing for data acquisition in the MIRA's scan mode, the greater the number of redundances for the 3-D image construction. However, shorter spacings imply a greater number of scan points and, consequently, making the survey time-consuming and increasing the equipment operation cost as well.

Regarding the MIRA equipment, field tests performed on the explore mode enable taking several arbitrary measurements (like dozens) in few minutes. Furthermore, the scan mode allows the pavement surface scanning to check the slab thickness uniformity, as well as the reinforcement and dowel bars positions.

2.2. Accuracy of MIRA tomographic device for concrete pavement applications

In recent years non standardized field tests were conducted to explore MIRA's inspection potential and accuracy on determining the thickness of pavement layers, dowel bars positioning

and covering of steel bars in continuously reinforced concrete pavements. Such device has become very popular for road construction control (including tunneling, bridges etc.).

In 2010, the United States Army Corps of Engineers (USACE) Engineer Research and Development Center (ERDC) was demanded by the United States Air Force (USAF) for the evaluation of several non-destructive methods for pavement thickness inspection, seeking to determine their capacity of estimating it accurately. Twelve different equipment for non-destructive evaluation were employed to assess forty experimental sections of hot mix asphalt (HMA) and Portland Cement Concrete (PCC) pavements in Vicksburg (USACE Experimental District, Mississippi). For calibration purposes, one core of the pavement surface layer was extracted by section (EDWARDS and MASON, 2011).

At the time, MIRA was the equipment with the best overall performance among those tested both for HMA and PCC, being the only equipment capable of measuring 100% of the PCC test sections with a mean error below 11 mm. The mean error for HMA layers was significantly higher (17,53 mm); however, just 43% of HMA sections were tested. Moreover, the equipment provided real-time measurements, stripping away the coring samples for equipment calibration, allowing its use in a completely non-destructive manner.

Figure 4 compares the PCC slabs thicknesses estimations with MIRA against the cored samples. It has been observed a high correlation (R^2 = 0,9932) and accuracy (slope = 0,9958) between the thickness measurements (ultrasonic *versus* cores).

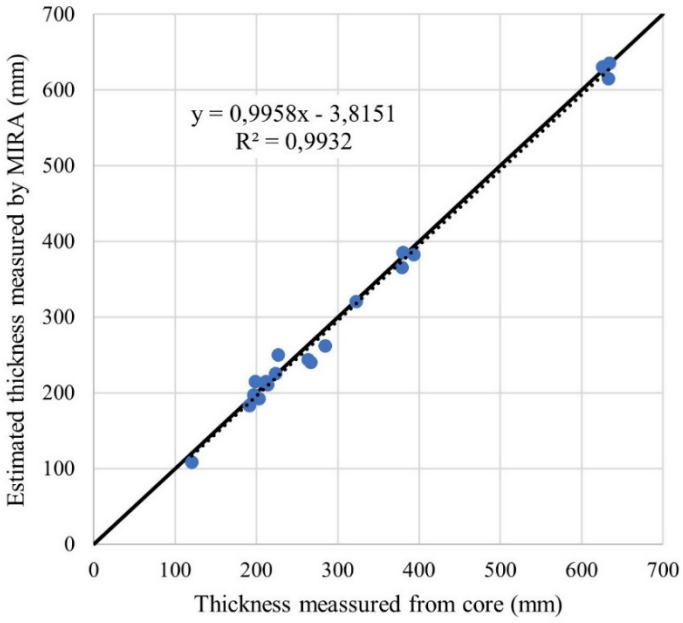

Figure 4. Comparison of thickness measured from by MIRA and those measured from core in PCC pavement sections (Adapted from Edwards and Mason, 2011).

Hoegh *et al*. (2011) present the results of field tests using MIRA for checking thickness and covering of the longitudinal steel reinforcement of a CRCP section. The equipment accuracy was evaluated from seven core samples extracted from the pavement for comparison with MIRA results.

Concerning the concrete highness over the steel reinforcement, results showed high correlation (R^2 = 0,991) and accuracy (slope = 0,972) for MIRA's measurements, with an

absolute mean error of 3,18 mm. Similarly, the comparison between the thickness results collected with MIRA *versus* the results measured from cores presented good correspondence (R^2 = 0,967) and accuracy (slope = 0.971).

Vancura *et al*. (2013) employed the MIRA to check the thickness of a jointed plain concrete pavement (JPCP) and compared the results with extracted cores. Two pavements newly built were inspected in a South District of Minnesota, with design thickness of 200 mm and 225 mm. For both the sections, twenty-three cores were extracted and 1,476 thickness measurements were performed.

Absolute mean error of the thickness measured with MIRA was 2,67 mm. In addition, the test results with MIRA have shown the data collected from cores did not capture the extreme peaks and valleys of the pavement thickness variation (at the slabs bottom) emphasizing that coring each 305 m (method adopted in the study) does not characterize the thickness variation properly.

Lybaert (2015) reports the use of MIRA in roads located at Ghent and Bekkevoort (Belgium) to check the dowel bars positioning in transverse joints of concrete slabs due to suspicions of construction problems impairing bars alignment. The results revealed the dowel bars misalignment along several joints. As an outcome, the author emphasizes that both the pavements were fully reconstructed, showing some road agencies in developed countries do not put up with some gross construction mistakes.

Van der Wielen *et al.* (2017) conducted tests on a newly built JPCP with 250 m length, 5 m width and concrete slab thickness of 200 mm laid on an asphalt base. The tests embraced thickness inspection and dowel bars position verification in the joints with ground penetrating radar (GPR) and ultrasonic tomography equipment (MIRA). Seeking to confirm the pavement thickness estimated through both the equipment, 142 leveling measurements were performed at referred points with total station (Leica iCON Robot 50), which, according to the authors, presents 1 mm of accuracy in estimating the elevations. The surface elevation at each reference point was measured before and after the concrete placement.

Regarding the pavement thickness measurements, the authors report that MIRA presented the best thickness estimation with a mean error of 3,52 mm (1,6% of relative error) and standard deviation of 2,35 mm. The best results with GPR were obtained with a 900 MHz antenna and calibrated speed, resulting in mean error of 4,05 mm (1,9% of relative error) and standard deviation of 3,19 mm.

Analyzing the dowel bar positioning, Van der Wielen *et al.* (2017) concluded that GPR works very well to pinpoint the dowel bars along the pavement section and, although the dowel bars might be successfully detected by MIRA, the method is less efficient than GPR due to the inability of continuous measurements.

3. MATERIALS AND METHODS

Located in the city of São Roque, São Paulo, Brazil, the private executive airport was designed years ago to receive national and international flights alleviating the demand of executive jets using Congonhas (São Paulo downtown airport) and Campo de Marte Airport. The referred airport has a main runway extension of 2,470 m and serves almost 120 private executive jets as parking and maintenance hub nowadays.

The airport hangar I apron was built using squared JCPC slabs of 4.8 m x 4.8 m and thickness of 180 mm, concrete with $f_{ct,f}$ = 4.5 MPa and dowel bars in any joint since airport pavements are submitted to a non-directional traffic, differing from bus corridors or roads channelized traffic. The slabs were placed on a CTCS base and well-graded crushed stone subbase, both 150 mm thick. Subgrade soil was a silt-clay with CBR = 8%.

The construction method used lateral forms comprising areas of 24 m by 24 m for concrete laying. One should note that the dowel bars were installed using a conventional steel basket for fixing the bars; once assembled such devices, with strong regards for bars parallelism and levelling, besides correct distance among them, were installed in the designed contraction joints positions, fixed over the cemented bases by using nail pistol with fasteners. No checking of vertical alignment of the dowel bar positions is actually done as a specification requirement since the standard for that (a road standard is used in Brazil, even for airport pavements) is lacking about such aspect.

Opposite requirements are mandatory in US since the Federal Aviation Administration lays down in the standard specification (FAA, 2018) that the dowel bars should be set up in the joints following the appropriate horizontal and vertical alignment. Accordingly, the dowel bars should be horizontally spaced within a range tolerance of 19 mm, whilst the vertical translations should not be greater than 12 mm. Additionally, the method applied to install the dowel bars must ensure that their horizontal and vertical misalignment is not higher than 2%.

About the method for spreading the base layer material, the FAA (2018) defines that cement-treated material should be spread with a mechanical spreader capable of receiving, spreading and shaping the mixture uniformly, avoiding segregation. The equipment should be supplied with a strike-off plate and gates capable of adjusting to the layer thickness and width. Equivalent regulations are present in Brazilian standards for compaction of road base materials, cemented or not.

Tests with MIRA were conducted in November 2019 a couple of days before its opening for landings and take-offs. The tests used MIRA's explore mode to analyze the slab thickness; for dowel bars positioning assessment the scan mode was employed. Twenty-five slabs were assessed with measurements taken at the slabs center for thickness checking. Regarding the dowel bars evaluation, data from two joints (one transverse and other longitudinal) of one slab were collected on the scan mode.

The data collection on the scan mode requires to mark an orthogonal grid line on the pavement surface to define the points where the equipment should be positioned allowing to achieve the desired information. Thus, after ensuring the joints are clean, the guidelines were marked on the pavement surface, as depicted in the Figure 5. Visibly it is a time-consuming procedure forbidding general check for all the pavement joints, requiring random approach in actual technological control procedure.

As the MIRA's effective aperture of the transducer's array is 250 mm, the spacing between lines should not surpass 250 mm. Additionally, the user manual recommends the grid lines should be spaced at a distance shorter than 250 mm at x-direction and shorter than 100 mm in the y-direction, related to the device movement on the pavement surface during the data collection. Thereby, it was taken a spacing of 200 mm in the x-direction and 100 mm in the y-direction, as depicted in the Figure 5b.

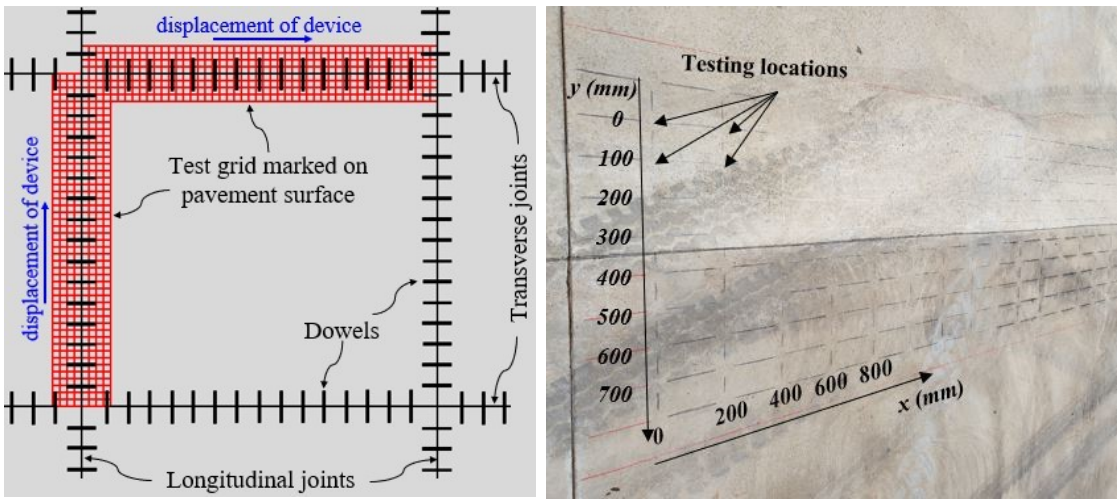

(a) Joints selected for data collection

(b) Guidelines marked on the pavement surface around the transverse joint

Figure 5. Delimitation of the guidelines for tests performed on the scan mode

In both the joints, eight lines in the x-direction and twenty-four in the y-direction were marked on the pavement surface. Thus, each joint surveyed resulted in 192 points of data acquisition with MIRA.

The equipment was set up in the scan mode for data acquisition at the minimum depth, which is 500 mm. After that, the software Idealviewer was used to reconstruct the mapped area which allows the 3-D visualization of scanned joints as well as the visualization of the tridimensional planes (B-scan, C-scan and D-scan) of the whole joint at the measurement's areas (Figure 6).

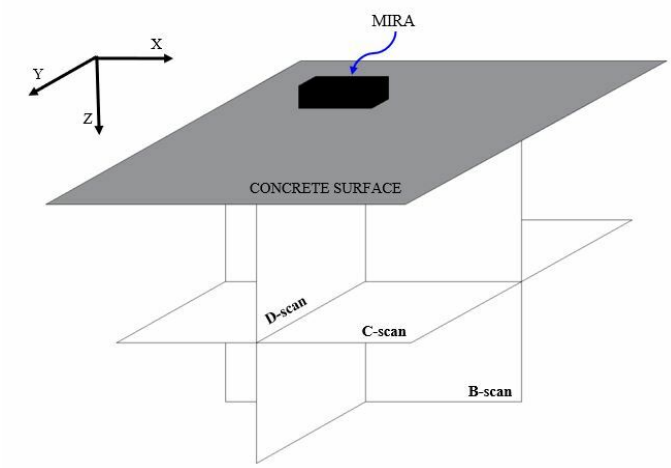

Figure 6. Tridimensional planes (B-scan, C-scan and D-Scan)

4. RESULTS AND DISCUSSIONS

4.1. Verification of the slabs thickness using the explore mode

Twenty-five slabs were selected to perform the survey on the explore mode, collecting information on the thickness at the center of the concrete slabs. Figure 7 depicts the B-scan obtained for one of the slabs where it is possible to observe a high intensity reflection (backwall) indicating the interface between the bottom of the concrete slab and the base layer.

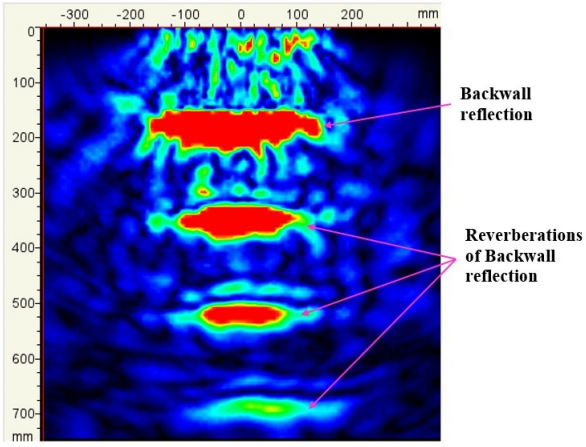

Figure 7. Example of B-scan centered at the concrete slab (explore mode)

The thickness obtained with MIRA's explore mode survey of slabs ranged from 151 mm to 222 mm; the average thickness was 172 mm with standard error of 2,95 mm and low coefficient of variation (8,6%). Results from descriptive statistics for a confidence level of 95% for the database are presented in the Table 2.

Table 2 – Statistics measurements of concrete slab thickness

Parameters	
Mean (mm)	172,16
Standard error (mm)	2,95
Median (mm)	175
Mode (mm)	175
Standard deviation (mm)	14,75
Kurtosis	4,34
Skewness	-0,578
Values range	71
Minimum value (mm)	151
Maximum value (mm)	222

The kurtosis positive result presented in Table 2 indicates a tailed distribution (leptokurtic), when compared to the normal distribution. Additionally, as the mean calculated is lower than the mode, the distribution is classified as asymmetric to the left. The asymmetry coefficient was calculated by the second Pearson's coefficient, and the asymmetry grade is considered moderate, as its module is in the range between 0.15 and 1.0.

The significant verified variations in the concrete slabs thickness in field compared to the design thickness result from the type of material and technique employed to spread the base, which does not ensure the flatness required for the base surface layer, leading to the concrete slab non-uniformity thickness. As well know by paving engineers experts only hot mix asphalt mixtures, as well as trowel finished concretes (no compacted ones) ensure flatness for the base surface.

4.2. Verification of the slab thickness and dowel bars alignment from the scan mode

Although the 3-D reconstruction (Figure 8) affords relevant information about the concrete slab thickness and uniformity, besides the image discontinuities which may characterize both the joint and a distress in the pavement structure, in such a visualization mode,

it is impossible precisely interpret the positioning and the dowel bars alignment conditions directly by the software Idealviewer.

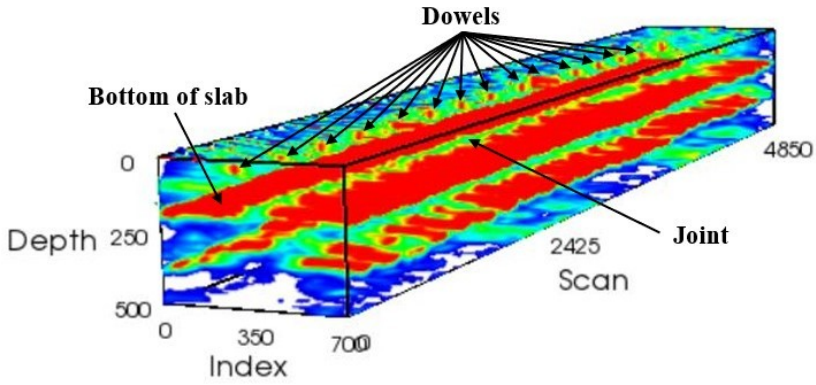

Figure 8. 3-D reconstruction of the transverse joint

Conversely, the software enables visualize the plane B-scan of the whole studied section at eight positions in the y-direction equally spaced from 100 mm, with four positions over each slab (split by the sawed contraction joint). Such a kind of visualization allows to check the slab thickness uniformity over the studied section, beyond enabling to check the dowel bars placement.

Thereby, to check the dowel bars alignment, the B-scans selected were “y = 200 mm” and “y = 500 mm”. As these positions are equidistant from joint, it was possible to visualize the dowel bars, even when small translations might have occurred.

Considering the dowel bars length, it normally ranges from 460 to 610 mm in airport pavements, according to FAA (2021), longitudinal translations higher than 50 mm can be verified from the other B-scans. However, if it is necessary to investigate minors’ longitudinal translations, spacing shorter than 100 mm should be considered for the device movement, which increases the results precision. In contrast, it demands a greater number of scan points on the pavement surface for the same survey area.

Dowel bars depth measurements (z) in the x-direction, in relation to the system origin (x, z) depicted in the B-scan images, were determined considering the reflection center which indicated the dowel bars presence.

Thereby, from dowel bars depth measurements on the B-scans “y = 200 mm” and “y = 500 mm”, the possible vertical tilt related to the project alignment was calculated employing basic trigonometry, admitting straight dowel bars. Similarly, the horizontal skew was calculated from determining the horizontal distance from the coordinate system (x, z).

The slab thickness was estimated drawing a line between the transverse section edges visualized on the images, and afterward the edge measurements were placed. Thus, the dowel bars positioning, as well as the slab thickness at the evaluated joints are depicted in the Figure 9 and Figure 10.

The slab thickness on the Figure 9a left side matches the Figure 10a right side, while the Figure 9b left side matches the Figure 10b right side, as schematically depicted in the Figure 5a, indicating the values obtained are the same as those obtained where the grid lines were overlapped to take the thickness measurements.

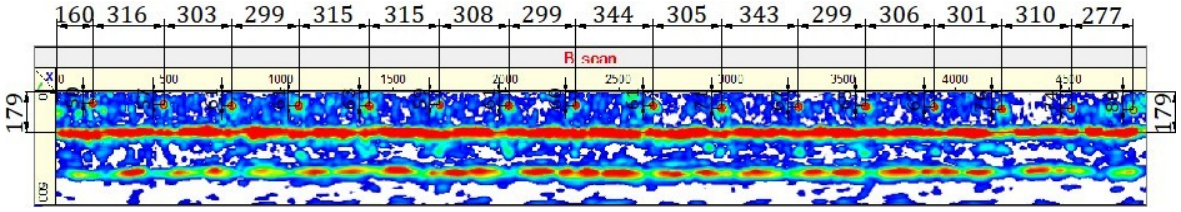

(a) B-scan at the alignment y = 200 mm

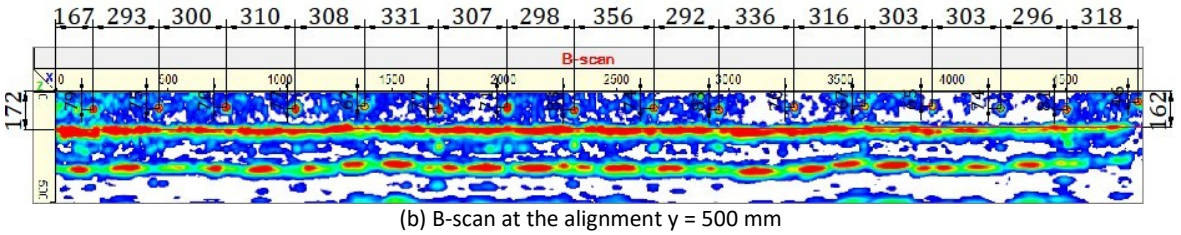

(b) B-scan at the alignment y = 500 mm

Figure 9. Verification of the slab thickness and dowel bars placement at the transverse joint

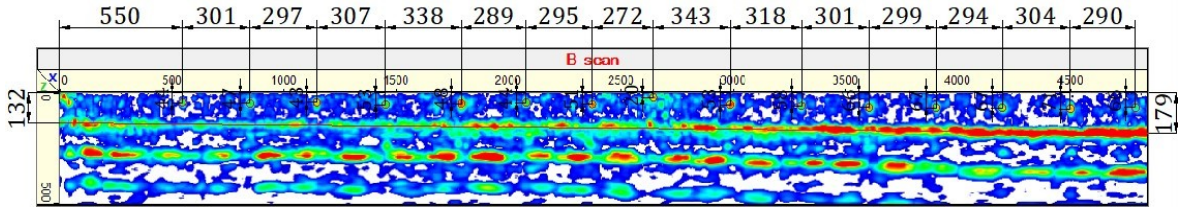

(a) B-scan at the alignment y = 200 mm

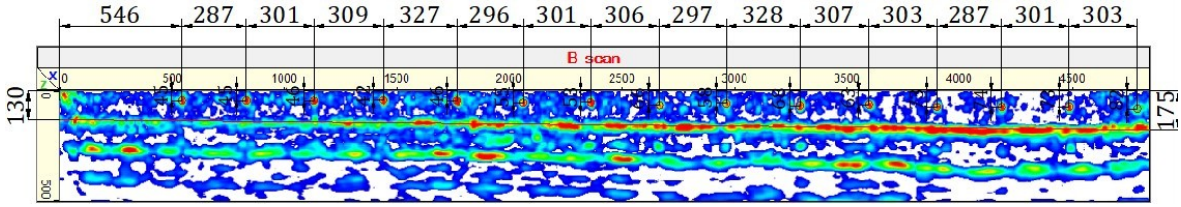

(b) B-scan at the alignment y = 500 mm

Figure 10. Verification of the slab thickness and dowel bars placement at the longitudinal joint

One should note on the longitudinal section B-scans (Figure 10a and Figure 10b) the slab thickness close to the left edge is about 130 mm, significantly (28%) lower than the 180 mm design thickness. This finding, aside from underlining the incidence of failures along pavement constructions control process, could bring consequences to the pavement performance, because, although it does not happen in a widespread way, slab thickness thinner than the designed one is a heavy concern for pavement performance.

The image backwall has shown important thicknesses variations, both transversal and longitudinal. Since concrete surface flatness is ensured buy constructive process, it is clear from the images that the cemented base surface is unlevelled even compaction densities achieved have met the specs. This is one aspect connected to the unevenness resulting after compaction of materials with no lubricant, whatever by type or amount, not capable of favoring the envelopment of aggregate grains.

Thickness negative variation are more concerning since both static as dynamic resistance of concrete slabs is hugely sensible to thickness, reducing drastically its fatigue life; or even jeopardizing a static rupture. This is explained by the fact that actual slab stresses, when thickness deficiency exists, can quite surpass the critical design stress, what induces non expected mechanical responses to load and curling.

Moreover, one can see in Figures 10a and 10b that the dowel bars height from the slab bottom remains practically the same along the whole extension, while the concrete cover decline as it is closer to the slab left edge, suggesting that the lack of uniformity in the concrete slab is probably related again to the base layer irregularity. It is also observed that, considering the joints sawing depth, which is generally 1/3 of the slab thickness (in this case, 60 mm), more than 50% of the dowel bars at the longitudinal joint are at an inadequate depth and, possibly, were partially or totally cut during the joint sawing operation.

It is worthwhile noting that the analyzed slab did not present lateral forms, just sawn joints; and, although it is impossible to affirm (since it is not known), likely, one of the joints is in the direction of the compaction roller, while the other one would be at the compaction perpendicular direction. Thus, there may be a sign that the compaction direction is constraint of a more sensible direction; in airport large areas the compaction process can differ a lot from highway construction.

Although the compaction direction is not matter of concern in road and bus corridors pavements due to constraint in the number of lanes, in case of airports, harbors and industrial areas, this aspect must be considered because of the slabs' significant dimensions (width and length).

Also, due the base layer unevenness, the thickness checking from a limited number of points (for instance, one or two points per concrete slab), even if carried out through non-destructive technique, tends not to be representative because of the inability of evidencing uniformity failures in the slab thickness.

Then, despite the results obtained with MIRA at the center of the inspected slabs, using the device explore mode, indicate a reasonable precision for slab thickness compared to the design, the sections obtained from the scan mode show the measures at the concrete slab center may not represent properly the real slab thickness.

In addition, it is possible to observe the lack of signal intensity where there should be a dowel bar in both the images (Figure 10a and Figure 10b). This might be associated to the dowel bar translation far away the joint (design position).

The vertical tilt and horizontal skew amplitudes related to the dowel bars design alignment conditions are presented in Tables 3 and 4. The negative signal indicated the dowel bars rotation on the opposite direction from that assumed as positive.

As can be seen from Table 3, at the transverse joint, 68,75% of the dowel bars do not present vertical or horizontal alignment within the tolerances established by the FAA (2018) standard. Analyzing the results for the longitudinal joint (Table 4), 43,75% of the dowel bars do not satisfy the limits set up for vertical tilt, while 75% of the dowel bars do not fulfill the horizontal skew tolerance.

Although the dowel bars misalignment may occur because of different reasons, the lack of suitable stiffness of metal baskets for bars support and how they are attached on the base layer are usually considered the critical factors when the bars are placed using such a technique. However, very stiff baskets could undermine stresses distributions and levels close to contraction joints, what must be analyzed carefully for a design decision.

Additionally, the lack of base layer surface flatness will affect the appropriate placement of the metal baskets, as discussed, impairing bars positioning due to twists and bends during the fixation, leading to dowel bars vertical tilt and horizontal skew from the original design position.

Table 3 – Dowel bars vertical tilt and horizontal skew at the transverse joints

	Depth z (mm)		Vertical tilt Amplitude		Distance from origin x (mm)		Horizontal skew Amplitude	
BT	y = 200mm	y = 500mm	Degree	%	y = 200 mm	y = 500 mm	Degree	%
1	50	79	5,521	9,667	160	167	1,337	2,333
2	57	75	3,434	6,000	476	460	-3,053	-5,333
3	61	70	1,718	3,000	779	760	-3,624	-6,333
4	61	77	3,053	5,333	1078	1070	-1,528	-2,667
5	63	67	0,764	1,333	1393	1378	-2,862	-5,000
6	59	77	3,434	6,000	1708	1709	0,191	0,333
7	61	71	1,909	3,333	2016	2016	0,000	0,000
8	60	83	4,384	7,667	2315	2314	-0,191	-0,333
9	61	74	2,481	4,333	2659	2670	2,100	3,667
10	71	83	2,291	4,000	2964	2962	-0,382	-0,667
11	67	70	0,573	1,000	3307	3298	-1,718	-3,000
12	65	67	0,382	0,667	3606	3614	1,528	2,667
13	67	65	-0,382	-0,667	3912	3917	0,955	1,667
14	76	74	-0,382	-0,667	4213	4220	1,337	2,333
15	74	81	1,337	2,333	4523	4516	-1,337	-2,333
16	80	46	-6,466	-11,333	4800	4834	6,466	11,333

Table 4 – Dowel bars vertical tilt and horizontal skew at the longitudinal joint

	Depth z (mm)		Vertical tilt Amplitude		Distance from origin x (mm)		Horizontal skew Amplitude	
BT	y = 200mm	y = 500mm	Degree	%	y = 200mm	y = 500mm	Degree	%
1	-	-	-	-			-	-
2	44	45	0,191	0,333	550	546	-0,764	-1,333
3	47	45	-0,382	-0,667	851	833	-3,434	-6,000
4	43	46	0,573	1,000	1148	1134	-2,672	-4,667
5	53	42	-2,100	-3,667	1455	1443	-2,291	-4,000
6	48	46	-0,382	-0,667	1793	1770	-4,384	-7,667
7	44	55	2,100	3,667	2082	2066	-3,053	-5,333
8	51	53	0,382	0,667	2377	2367	-1,909	-3,333
9	20	66	8,717	15,333	2649	2673	4,574	8,000
10	53	58	0,955	1,667	2992	2970	-4,194	-7,333
11	58	68	1,909	3,333	3310	3298	-2,291	-4,000
12	66	63	-0,573	-1,000	3611	3605	-1,146	-2,000
13	67	73	1,146	2,000	3910	3908	-0,382	-0,667
14	67	74	1,337	2,333	4204	4195	-1,718	-3,000
15	71	73	0,382	0,667	4508	4496	-2,291	-4,000
16	66	82	3,053	5,333	4798	4799	0,191	0,333

5. CONCLUSIONS

Several field non-destructive tests using the MIRA ultrasonic low frequency waves device were performed at an apron in an executive airport site, over a newly built JPCP.

The tests were carried out considering two operation modes available in the device: the explore mode that enables to perform the tests at arbitrary positions (here, centered at the concrete slabs inspected); and the scan mode, used to create a folder to store the database generated from a complete surface scanning (joints region mapping) to later 3-D reconstruction.

A total of twenty-five concrete slabs were inspected using the explore mode to check their thickness and one concrete slab was selected to map two of its joints using the scan mode to check the slab thickness along the joint as well as the dowel bars placement compliance.

Regarding results from explore mode, it is revealed an important variability in concrete slab thickness, ranging between 151 mm and 222 m, with average of 172 mm and coefficient of

variation of 8,6%. These results are closely related to the employment of inappropriate techniques and equipment which do not ensure the base layer surface evenness, resulting in non-uniformity of the concrete slabs thickness.

Then, albeit using the equipment on the explore mode allow to reach a good productivity in determining the concrete slabs thickness, because of the base layer irregularity the slab thickness verification from a limited number of points (as performed in this study) may not be representative; it is required a significant number of tests at the same slab for a suitable checking of concrete slab uniformity and thickness or through the slab sections scanning (transverse and longitudinal).

The tests carried out on the scan mode allowed to survey the pavement surface verifying slab thickness uniformity, as well as the dowel bars placement. The results show the slab thickness non-uniformity surrounding both the transverse and longitudinal joints. From longitudinal section B-scans it was possible to observe the thickness at the edge of the investigated slab was 28% slightly thinner than the design. Additionally, more than 50% of the dowel bars at the assessed longitudinal joint had some wander related to slab depth. However, such aspects should be taken as built-related scatter mainly due to unevenness of the base surface (lack of flatness).

Most of the dowel bars at both the joints assesses presented misalignment higher than the FAA tolerances. However, it is relevant to highlight these tolerances are not usually based on performance data.

Furthermore, the excessive lack of flatness over the base layer surface can affect the bars alignment during the fixation of the metal baskets, due the risk of bending and twisting of such devices. Therefore, controlling the vertical geometric levelling of the base layer contributes to mitigate variations in the slab thickness uniformity and to ensure the bars alignment when dowel baskets are used as well.

Therefore, as main conclusion, since base types are a design decision, it is strongly recommended the use of special baskets permitting vertical adjustments of the bars levels ensuring al of then (in one joint) shall be at the same covering distance from the finished concrete surface.

Ultimately, the use of non-destructive evaluation methods which enable partially scan the pavement surface like is the case of MIRA, trends to contribute to analysis that allows to check, among other parameters, the thickness uniformity along the pavement sections, besides the positioning of reinforcement and dowel bars.

From the investigated sections B-scans it was possible to check the dowel bars vertical and horizontal misalignments, underlining the potential of using MIRA for checking the dowel bars placement compliance for in service pavements.

ACKNOWLEDGEMENTS

The authors thank CAPES - Ministry of Education - for the doctoral scholarships granted to the first and third author. Also are grateful to São Paulo Catarina International Airport for permission to publish the collected data.

REFERENCES

American Concrete Pavement Association - ACPA (2006). *Evaluating and optimizing dowel bar alignment*. American Concrete Pavement Association. Concrete Pavement Research and Technology – Special Report, Rosemont.

American Concrete Pavement Association - ACPA (2013). *Dowel bar alignment and location for placement by mechanical dowel bar insertion*. American Concrete Pavement Association. Guide specification. Skokie.

Aguirre, O., Vidaud, I., Peña, L., Vidaud, E. (2013). Evaluación de integridad estructural mediante tomografía tridimensional ultrasónica (MIRA). *Construcción y Tecnología en Concreto*, p. 24-28. Available at: <http://www.germann.org/TestSystems/MIRA%20Tomographer/MIRA-IMCYC%20parte%202.pdf.>. Access: 22.02.2022.

Balbo, J. T. (2014). "Bases asfálticas para pavimentos de concreto: to biuld or not to build?". *Revista Pavimentação*, v. 31, p. 31-45 (in Portuguese).

Departamento Nacional de Infraestrutura de Transportes (2013). *Pavimento rígido – Execução de pavimento rígido com equipamento de fôrma-deslizante*. Departamento Nacional de Infraestrutura de Transportes. Norma DNIT 049/2013-ES. Especificação de serviço. Instituto de Pesquisas Rodoviárias, Rio de Janeiro (in Portuguese).

Edwards, L.; Mason, Q. (2011). *Evaluation of nondestructive methods for determining pavement thickness*. U.S. Army Engineer Research and Development Center – Geotechnical and Structures Lab. Final Report – ERDC/GSL TR-11-41. Vicksburg.

Federal Aviation Administration (2018). *Standard specification for construction of airports*. U. S. Department of Transportation. Federal Aviation Administration. Advisory Circular: 150/5370-10H, Washington, DC. Available at: https://www.faa.gov/documentLibrary/media/Advisory_Circular/150-5370-10H.pdf. Access: 13.07.2022.

Federal Aviation Administration (2021). *Airport pavement design and evaluation*. U. S. Department of Transportation. Federal Aviation Administration. Advisory Circular: 150/5320-6G, Washington, DC. Available at: https://www.faa.gov/documentLibrary/media/Advisory_Circular/150-5320-6G-Pavement-Design.pdf. Access: 13.07.2022.

Federal Highway Administration (2007). *Best practices for dowel placement tolerances*. Federal Highway Administration. Tech Brief – Concrete Pavement Technology Program, HIF-07-021, Washington.

Federal Highway Administration (2019). *Concrete pavement joints*. Federal Highway Administration. Technical Advisory, T 5040.30, Washington.

Gancarz DJ, Tayabji SD, Vavrik WR. (2015). Testing of Dowel Alignment and Development of a Dowel Bar Alignment Specification for Illinois Tollways. *Transportation Research Record.* n. 2504(1):117-123. DOI:10.3141/2504-14.

Germann Instruments (2016). *MIRA™ Low-frequency ultrasonic tomographer*. Operation Manual. Copenhagen.

Hoegh K, Khazanovich L, Yu HT. (2011). Ultrasonic tomography for evaluation of concrete pavements. *Transportation Research Record*. n. 2232(1):85-94. DOI:10.3141/2232-09.

Hoegh K, Khazanovich L, Yu HT. (2012). Concrete pavement joint diagnostics with ultrasonic tomography. *Transportation Research Record*. n. 2305(1):54-61. DOI:10.3141/2305-06.

Lybaert, M. (2015). *Ultrasonic tomography, a non-destructive measuring technique for analysis of concrete roads*. Belgian Road Research Centre. Available at: https://ectri.org/static/YRS15/Documents/Papers&presentations/Session%202B%20Transport%20Civil%20&%20Road%20Engineering/Papers/Ultrasonic_tomography,_a_non-destructive_measuring_technique_for_analysis_of_concrete_roads_LYBAERT.pdf.. Access: 2.02.2022.

Parmenter, B. S. (1973). The design and construction of joints in concrete pavements. *Transport and Road Research Laboratory* – TRRL Report LR 512, Berkshire.Rao, S., Hoegh, K., Yu, H. T., Khazanovich, L. (2009). Evaluation of dowel constructability in Portland cement concrete pavements. Journal of the *Transportation Research Board*, n. 2098, p. 86-93. doi: 10.3141/2098-09.

Schickert M, Krause M, Müller W. (2003). Ultrasonic imaging of concrete elements using reconstruction by synthetic aperture focusing technique. *Journal of Materials in Civil Engineering*;15(3):235–46. http://dx.doi.org/10.1061/(ASCE)0899-1561(2003)15:3(235).

Sturges, T., Frankhouser, A., Abbas, A. R. (2014). Evaluation of dowel bar alignment from a two-step dowel bar insert. *International Journal of Pavement Engineering*, Vol. 15, N° 5, 438-448. DOI: 10.1080/10298436.2013.815354.

Tayabji, S. D. (1986). Dowel placement tolerances for concrete pavements*. In: Transportation Research Record 1062*, TRB, National Research Council, p. 47-54, Washington, D.C, USA.

Vancura, M.; Khazanovich, L.; Barnes, R. (2013). Concrete pavement thickness variation assessment with cores and nondestructive testing measurements. *Transportation Research Record*, v. 2347, n. 1, p. 61-68, 2013. DOI: 10.3141/2347-07

Van der Wielen, A.; Lybaert, M.; Grégoire, C. (2017). Combined GPR and ultrasonic tomography measurements for the evaluation of a new concrete pavement. *In: 2017 9th International Workshop on Advanced Ground Penetrating Radar (IWAGPR)*. IEEE, 2017. p. 1-6.